BASIC RESEARCH

# Vimentin and laminin are altered on cheek pouch microvessels of streptozotocin-induced diabetic hamsters

**Jemima Fuentes R. Silva,[I] Fatima Z. G. A. Cyrino,[III] Marisa M. D. Breitenbach,[II] Eliete Bouskela,[III] Jorge José Carvalho[I]**

[I]Universidade do Estado do Rio de Janeiro, Laboratory of Cellular Ultrastructure and Tissue Biology, Biomedical Center, Institute of Biology, Rio de Janeiro/RJ, Brazil. [II]Universidade do Estado do Rio de Janeiro, Department of Physiological Sciences, Biomedical Center, Rio de Janeiro/RJ, Brazil. [III]Universidade do Estado do Rio de Janeiro, Clinical and Experimental Research Laboratory on Vascular Biology (BioVasc), Biomedical Center, Rio de Janeiro/RJ, Brazil.

**OBJECTIVES:** Normal endothelial cells respond to shear stress by elongating and aligning in the direction of fluid flow. Hyperglycemia impairs this response and contributes to microvascular complications, which result in deleterious effects to the endothelium. This work aimed to evaluate cheek pouch microvessel morphological characteristics, reactivity, permeability, and expression of cytoskeleton and extracellular matrix components in hamsters after the induction of diabetes with streptozotocin.

**METHODS:** Syrian golden hamsters (90–130 g) were injected with streptozotocin (50 mg/kg, i.p.) or vehicle either 6 (the diabetes mellitus 6 group) or 15 (the diabetes mellitus 15 group) days before the experiment. Vascular dimensions and density per area of vessels were determined by morphometric and stereological measurements. Changes in blood flow were measured in response to acetylcholine, and plasma extravasation was measured by the number of leakage sites. Actin, talin, $\alpha$-smooth muscle actin, vimentin, type IV collagen, and laminin were detected by immunohistochemistry and assessed through a semiquantitative scoring system.

**RESULTS:** There were no major alterations in the lumen, wall diameters, or densities of the examined vessels. Likewise, vascular reactivity and permeability were not altered by diabetes. The arterioles demonstrated increased immunoreactivity to vimentin and laminin in the diabetes mellitus 6 and diabetes mellitus 15 groups.

**DISCUSSION:** Antibodies against laminin and vimentin inhibit branching morphogenesis in vitro. Therefore, laminin and vimentin participating in the structure of the focal adhesion may play a role in angiogenesis.

**CONCLUSIONS:** Our results indicated the existence of changes related to cell–matrix interactions, which may contribute to the pathological remodeling that was already underway one week after induction of experimental diabetes.

**KEYWORDS:** Diabetes Mellitus; Microcirculation; Cytoskeleton; Extracellular Matrix; Immunohistochemistry.

Silva JFR, Cyrino FZGA, Breitenbach MMD, Bouskela E, Carvalho JJ. Vimentin and laminin are altered on cheek pouch microvessels of streptozotocin-induced diabetic hamsters. Clinics. 2011;66(11):1961-1968.

**Received for publication on** April 2, 2011; **First review completed on** May 19, 2011; **Accepted for publication on** July 11, 2011

E-mail: jjcarv@gmail.com

Tel.: 55 21 2587-6135

## INTRODUCTION

The microcirculation represents a unique environment that acts as the site of gas and nutrient exchange between blood and tissues.[1] Microvessel networks are often idealized as a set of vessels of different categories that are connected in a series with the parallel vessels in each category exhibiting identical properties.[1] In reality, however, the structures of microvessel networks are highly heterogeneous. This heterogeneity has important effects on the functional behavior of the microcirculation.[2] Consequently, the physiology, biochemistry, and pharmacology vary according to the portion of the network that is studied and the location within different tissues.[1]

Diabetes mellitus is caused by physical or functional loss of beta-cell mass, which results in hyperglycemia. In turn, hyperglycemia contributes to microvascular complications, which result in deleterious effects on the endothelium. Endothelial and smooth muscle cells are largely responsible for regulating vascular tone and permeability, and they make up the subendothelial matrix. Endothelial dysfunction



No potential conflict of interest was reported.

is regarded as an important factor in the pathogenesis of microangiopathy.[3]

Numerous hyperglycemia-related mechanisms have been hypothesized to mediate micro- and macrovascular complications. These mechanisms include the polyol and hexosamine pathways, protein kinase C (PKC) activation, generation of reactive oxygen species, poly(ADP-ribose) polymerase (PARP) activation, and the accumulation of advanced glycoxidation or glycation end-products (AGEs).[4]

Microvascular deterioration in diabetes has been associated with increased blood flow, venular dilation, basement membrane thickening, increased exudation of plasma proteins, decreased density of microvessels, and decreased oxygen supply to the tissues.[5]

Several investigators have described an increase in microvascular permeability[6] and changes in endothelium-dependent relaxation[7] in streptozotocin (STZ)-induced diabetic animals during the prediabetic period (six–eight weeks). These changes could be due to increased intravascular pressure, which occurs as a result of the increased shear stress on the vascular luminal surface,[8] and the accumulation of extracellular matrix and cytoskeleton proteins glycated by AGEs.[9] The regulation of these processes occurs via the mechanically stimulated release of potent, shear-responsive, endothelial-derived factors, such as nitrovasodilators, prostaglandins, lipoxygenases, hyperpolarizing factors, growth factors.[10]

In contrast to vessel changes observed during acute vasoregulation, sustained changes in the local hemodynamics promote the adaptive structural remodeling of the arterial wall through endothelium-dependent regulation of gene and protein expression.[11] Moreover, morphologic alteration of arterioles, capillaries, and venules has been demonstrated after chronic hyperglycemia in diabetic human subjects, rats, and mice.[12]

Prolonged hyperglycemic states result in the generation of reactive oxygen species, which leads to morphological changes in response to endothelial dysfunction.[13] These morphological changes ultimately require the dynamic cytoskeleton and its interaction with the extracellular matrix (ECM).[14]

Most previous analyses of microvessels in the hamster cheek pouch model and other animal models have been performed after a period of two weeks from the development of diabetes.[5,6] Early alterations (first two weeks) in the microvasculature that may contribute to the onset and progression of type 1 diabetes, however, remain elusive. Thus, an integrated analysis of the structural and physiological parameters of the microcirculation during the first two weeks of diabetes development is necessary.

The main purpose of this work was to qualitatively describe the structural alterations that occur in microvessels and in the cytoskeleton and ECM components during the early stage of diabetes mellitus development. In addition, we wanted to study the sensitivity of the microvascular membrane to histamine and the endothelium-dependent relaxation induced by acetylcholine.

## MATERIALS AND METHODS

### Animals and Induction of Diabetes Mellitus

The study protocol was approved by the Ethics Committee for Experimental Animals, no. CEA 004/2009, of the State University of Rio de Janeiro, Brazil. All procedures were carried out in accordance with the conventional guidelines for experimentation with animals. Twenty-four male Syrian golden hamsters (*Mesocricetus auratus),* seven to ten weeks old and weighing 90-130 g, were maintained in separate cages under controlled temperature and humidity and a 12/12 h light/dark cycle. Animals had free access to food and water.

Syrian golden hamsters were randomly divided into a control group (CG) and a diabetic group. Experimental type 1 diabetes mellitus was induced by intraperitoneal (i.p.) injections of STZ (50 mg/kg body weight/day, Sigma Chemical Co., St. Louis, MO, USA) dissolved in 50 mmol/l sodium citrate buffer (pH 4.5) for three consecutive days (a total dose of 150 mg/kg) at intervals of 24 h. Hamsters in the CG (n = 8) received sodium citrate buffer alone. Diabetic animals were further divided according to the duration after STZ administration: 6 days (n = 8; DM6) or 15 days (n = 8; DM15) of diabetes development. Before the STZ injection and at 1 h, 24 h, and 3, 6, and 15 days after the last injection, postprandial blood glucose and body mass were measured to confirm diabetes (≥210 mg/dl). Three days after the last STZ injection, the diabetic condition was confirmed. Only animals showing weight loss (due to uncontrolled diabetes) and severe hyperglycemia were considered for the analyses.

### Intravital Microscopy of the Hamster Cheek Pouch

Hamsters from each group were prepared for intravital microscopy according to the methods described in Svensjö (1999)[6] at 6 or 15 days after the STZ treatment. Animals were anesthetized with an injection of sodium pentobarbital (60 mg/ml, i.p.) supplemented with i.p. dose of α-chloralose (100 mg/kg) through a femoral vein catheter, and body temperature was kept at 36.5°C. To facilitate spontaneous breathing, a tracheostomy was performed. The right femoral vein was cannulated for the administration of fluorescein-dextran (FITC–dextran, MW 150,000, TdB Consultancy, Uppsala, Sweden), which was used to measure the restrictiveness of the microvascular membrane permeability. Alterations in the postcapillary venular permeability were measured using semiquantitative methods by counting sites with extravasation of fluorescent plasma (leaky sites = leaks) at 0, 2, and 5 min after the topical application of histamine ($10^{-6}$ mol). To determine the vascular reactivity, the luminal diameter of selected arterioles and venules (40-90 μm) was measured both before and 10 min after the microapplication of acetylcholine ($10^{-4}$ mol, micropipette 10-12 μm and constant volume of 200 μl/min). Microvessels were analyzed using a millimetric ocular lens of a light microscope and observed with a computer-assisted method on analog–digital-converted, video-recorded images. To avoid bias due to single-operator measurements, two independent blinded operators measured vessel diameters.

### Morphometric and Stereologic Analysis

To reduce measurement errors, intimal (IL) and media layers (ML) were analyzed by different techniques. To determine the thickness of the IL, the cheek pouch was fixed in 2.5% glutaraldehyde and 2.0% paraformaldehyde in 0.15 M cacodylate buffer (pH 7.2) for 2 h. The IL was then postfixed in 1% osmium tetroxide, stained in 2% uranyl acetate, dehydrated in acetone, and embedded in epoxy resin (Epon-812, SEM, Hatfield, PA, USA). Thin sections (1 μm thick) were stained with 0.25% toluidine blue in 1% acetic acid (Vetec, Brazil) and observed under a light

microscope (Axiophot, Carl Zeiss, Germany). Media layer thickness was determined using light microscopy with immunolabeling for α-smooth muscle actin (α-SMA). For details on immunohistochemistry, please see section ''Immunohistochemistry Assay''.

The digital images of 20 vessels for each hamster (TIFF format, 36-bit color, 1,280 X 1,024 pixels) were acquired using a 100X oil-immersion objective lens and manually quantified with the Image-Pro Plus 4.5 program (Image Pro Plus 4.5, Media Cybernetics, Bethesda USA). This sample size was based on previous studies and was designed to avoid biases related to inter-animal variability.[15,16]

Vascular dimensions were measured taking into account three parameters: lumen diameter, wall thickness and wall/lumen ratio. We obtained four measurements of IL and ML thickening (i.e., at 0°C, 90°C, 180°C and 270°C). The luminal area was measured from the internal circumferential line, and the lumen diameter was calculated from the area. The percentage of thickening was measured by the lumen/wall ratio.[17] It is important to highlight that the lumen diameter, wall thickness and lumen/wall ratio measurements in hamsters were obtained from a previous work,[5] and the measures from the previous study were used as a pattern for the species.

The volume density was analyzed by stereology using a test system composed of 36 test points ($P_T$)[15] and estimated by the following equation: Vv [structure] = *P*p [structure]/*P*t, where *P*p is the number of points that hit the structure, and *P*t is the total number of test points inside the test system. The density per area was estimated for vessels (arterioles or venules) with the following equation: $Q_A$[structure] = *N*[structure]/$A_T$ (1 $mm^2$), where *N* is the number of profiles counted in the test area (i.e., the frame $A_T$), considering the forbidden line and its extensions.[15]

### Immunohistochemistry Assay

Paraffin sections of cheek pouches were deparaffinized, rehydrated, and incubated (10 min) with 0.3% $H_2O_2$ in methanol to block endogenous peroxidase. Nonspecific protein binding was blocked by incubation with 1% bovine serum albumin diluted in phosphate-buffered saline (PBS/BSA). Antigen retrieval for ECM components was performed with trypsin (3%) diluted in distilled water for 10 min at 37°C and the sections were incubated with the primary antibody diluted 1:100 with 1% PBS/BSA overnight (4°C, in a humid atmosphere). Cytoskeleton protein sections were incubated in 10 mM sodium citrate buffer (pH 6.0, Antigen Unmasking Solution, H-3300; Vector Laboratories, CA, USA) at 98°C for 20 min and subsequently incubated with the primary antibody diluted 1:25. After washing with PBS, slides were incubated with reagent from the Labeled Streptavidin-Biotin System (LSAB) immunohistochemical kit (LSAB-kit, Dako, Carpinteria, CA). Sections were then counterstained with hematoxylin and mounted using an aqueous mounting medium. Control sections were processed after the omission of the primary antibody. Immunohistochemistry staining was evaluated based on a semiquantitative scoring system: score 0, no label; score 1, poor label; score 2, medium label; score 3, strong label.[16]

### Data Analysis

All data are presented as the mean ± the standard error of the mean (SEM) and tested with one-way ANOVA followed by Tukey's test, using the GraphPad Prism program (5.0 version, GraphPad Software San Diego, USA). In all cases, $p<0.05$ was considered statistically significant.

## RESULTS

### Effects of STZ-Induced Diabetes on Body Weight and Morphofunctional Parameters

As expected, glycemia was extremely high in the hamsters in the diabetic groups. The hamsters were only persistently hyperglycemic after the third day after STZ administration. Compared with the CG, glycemia was increased two-fold in diabetic hamsters 6 days (DM6) after STZ administration and increased almost three-fold in diabetic hamsters 15 days (DM15) after the induction of diabetes ($p<0.001$ for the CG vs. DM6 and DM15). The degree of glycemia was also different between DM6 and DM15 ($p<0.05$, Figure 1A). In addition, diabetic hamsters suffered a significant reduction in body weight. The control group showed a weight gain of approximately 5% from day 0 to day 6, whereas the DM6 hamsters displayed a loss in body weight of around 15% for the same time period ($p<0.05$ for the CG vs. DM6). DM15 hamsters lost 20% compared with the control ($p<0.001$ for the control group vs. DM15) (Figure 1B).

There were significant differences ($p<0.05$) in the microvascular permeabilities of both the diabetic subgroups (105±3 and 112±8 leakage sites/$cm^2$ for the DM6 and DM15 groups, respectively) compared with the control group (158±13 leakage sites/$cm^2$) 2 min after the end of the topical application of histamine. The peak vascular response, however, usually occurred at 3 to 5 min after the application and dissipated within 10 or 20 min (data not shown). Responses were not significantly different between any two groups at 5 min ($p>0.05$, Figure 1C). For acetylcholine, there were no significant differences between the diabetic and control hamsters in any determination for any vessel tested (arterioles or venules) ($p>0.05$ for comparison between groups, Figure 1D).

Table 1 shows that no significant differences between groups were observed for morphometric or stereological parameters. Microvessel density per cheek pouch area (QA) and volume density (Vv) were estimated to determine the amount of cheek pouch vascularization in age-matched control and diabetic hamsters. For both parameters, the number of venules was two times greater than the number of arterioles, but no significant difference between groups was observed in any analysis ($p>0.05$).

### Immunohistochemistry Score

Actin expression increased in arterioles of the DM6 hamsters compared with the CG. DM15 hamsters do not alter actin expression compared with the CT but showed decrease compared with the DM6 hamsters (CG, score 1; DM6, score 2; DM15, score 1). Actin immunoreactivity was seen in all endothelial and smooth muscle cells (data not shown). There is no difference in actin or talin immunostaining in venules between the groups. The α-SMA immunostaining in arterioles do not change between the groups. In arterioles, talin immunostaining showed an increase in DM6 hamsters when compared to control hamsters. Talin-positive vessels decreased in DM15 hamsters when compared to DM6 hamsters and there is no different relationship with the control group (CG, score 1; DM6, score 3; DM15, score 1). Immunoreactivity for talin was positive in endothelial cells and smooth muscle cells (data not

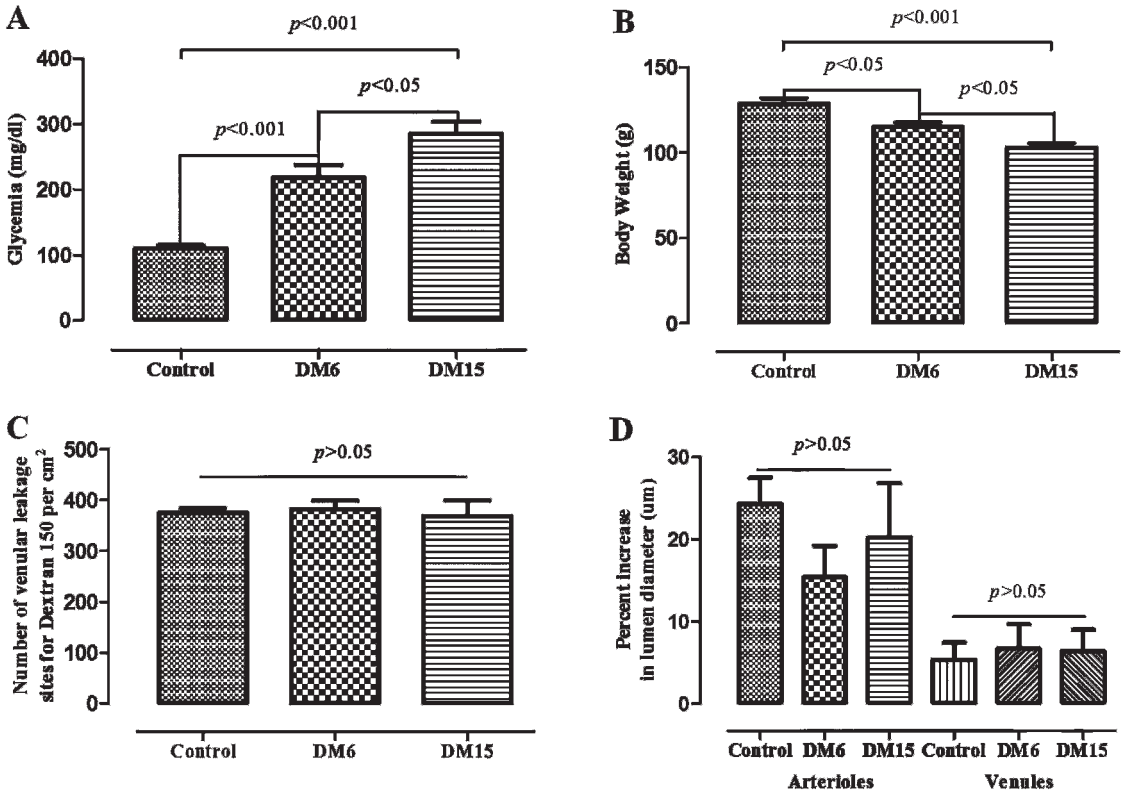


**Figure 1 -** The mean ± the standard error of the mean (SEM) for glycemia, body weight, and microvascular responses to histamine and acetylcholine in age-matched controls and hamsters at 6 (DM6) and 15 days (DM15) after the induction of diabetes with streptozotocin (STZ, 50 mg/kg). Statistical significance was determined using one-way ANOVA followed by Tukey's post-hoc analysis. **A**. Glycemia (mg/dl): $p<0.001$ for the control group vs. both DM6 and DM15, and $p<0.05$ for the DM6 group compared with the DM15 group. **B**. Body weight (g): $p<0.05$ for the control group vs. the DM6 group, $p<0.001$ for the control group vs. the DM15 group, and $p<0.05$ for the DM6 group vs. the DM15 group. **C**. Microvascular responses (number of dextran 150kDa leakage sites per $cm^2$) to histamine ($10^{-6}$ M). There were no significant differences between the groups ($p>0.05$). **D**. Responses (as percent increase in lumen diameter) of arterioles and venules to topical application of acetylcholine. There were no significant differences between the groups ($p>0.05$).

shown). α-SMA expression in venules was increased in the DM6 hamsters compared with the control and the DM15 hamsters (CG, score 1; DM6, score 3; DM15, score 1). Vimentin-positive arterioles and venules increased in DM6 and DM15 hamsters when compared to control hamsters (CG, score 1; DM6, score 2; DM15, score 2). In the CG, the anti-vimentin antibody only reacted with some endothelial cells, but immunoreactivity was also apparent in smooth muscle cells in both of the diabetic groups. Furthermore, a greater number of cells stained positively for vimentin in the DM6 and DM15 groups compared with the CG (Figure 2).

The expression of laminin was more apparent in hamsters in the first week after STZ induction of diabetes than in the control hamsters. Laminin labeling was maintained for 15

**Table 1 -** Morphological and stereological measurements of microcirculatory vessels of age-matched control and diabetic hamsters.

| Measurements/Groups/Vessels | Control | | 6 days of diabetes | | 15 days of diabetes | |
|---|---|---|---|---|---|---|
| | Arterioles | Venules | Arterioles | Venules | Arterioles | Venules |
| ***Thickness of the intimal and media layers (μm)*** | | | | | | |
| *Lumen diameter* | 31±2.7 | 40±3 | 33±1.2 | 42±2.4 | 25±2.5 | 35±3.1 |
| *Wall thickness* | 5.7±0.7 | 3.6±0.6 | 5.4±0.9 | 2.7±0.4 | 3.8±0.4 | 2.4±0.2 |
| *Wall/lumen ratio* | 0.2 0 | 0.1 0 | 0.2 0 | 0.1 0 | 0.2 0 | 0.1 0 |
| ***Thickness of the media layer (μm)*** | | | | | | |
| *Lumen diameter* | 38±3.7 | 41±2.4 | 30±3.8 | 32±2.1 | 28±7.4 | 39±5.4 |
| *Wall thickness* | 5.3±0.3 | 2.6±0.2 | 5.4±0.2 | 2.5±0.1 | 5±0.8 | 2.4±0.1 |
| *Wall/lumen ratio* | 0.1 0 | 0.1 0 | 0.2 0 | 0.1 0 | 0.2 0 | 0.1 0 |
| ***Density per cheek pouch area (QA) ($\mu m^2.10^2$)*** | | | | | | |
| *QA* | 3.2±0.7 | 8.8±1.3 | 3.2±0.5 | 7.2±1 | 3.5±0.7 | 9.7±1 |
| ***Volume density (Vv) (%)*** | | | | | | |
| *Vv* | 5.5±1.3 | 11±1.5 | 5.3±1.1 | 11±1.6 | 5.2±1.4 | 10±1.9 |

**Values are the mean±the standard error of the mean. *p*-values are not significant for any data measured.**

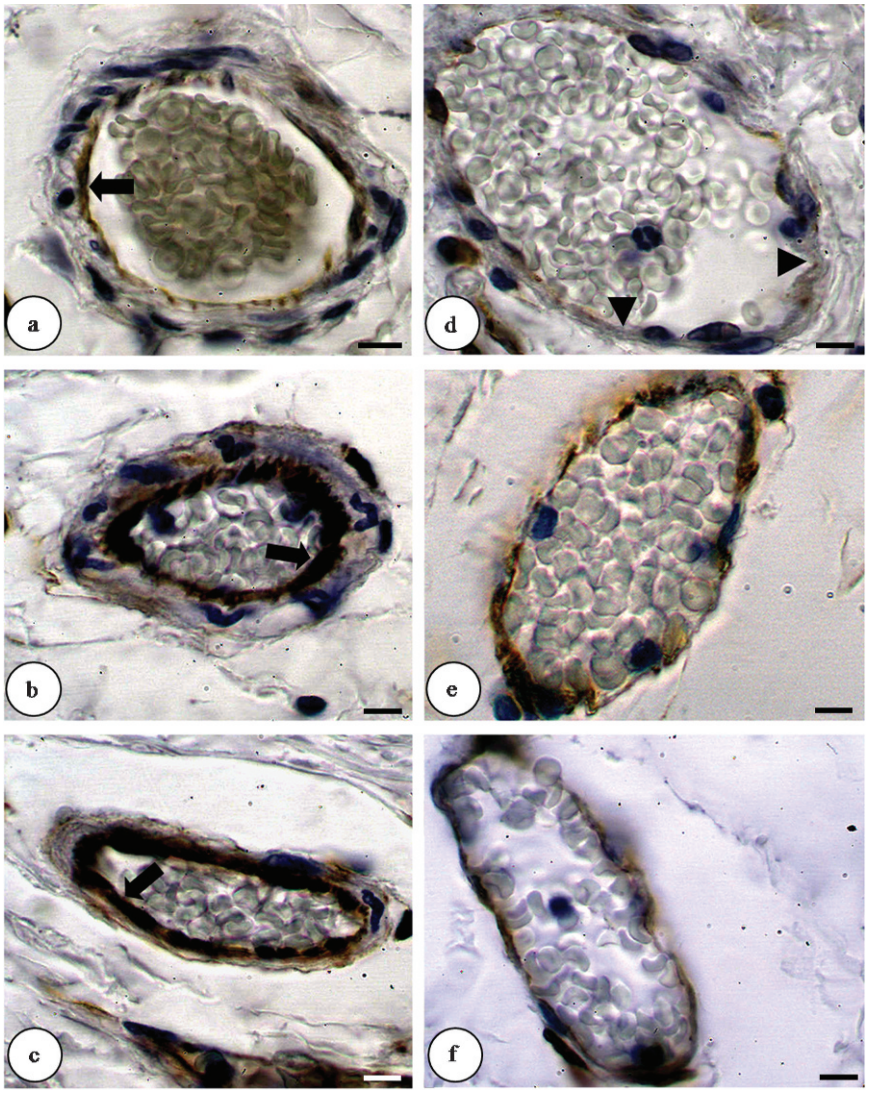


**Figure 2 -** Changes of vimentin expression in arterioles (A-C) and venules (D-F) by immunohistochemical staining (brown color) (light microscopy, 1,000X). **a**. The control group only showed a few vimentin-immunoreactive endothelial cells (arrow). **b**. The diabetic group (6 days) showed positively-stained endothelial (arrow) and smooth muscle cells. **c**. The diabetic group (15 days) showed vimentin-immunoreactive endothelial (arrow) and smooth muscle cells. **d**. The control group with few endothelial cells immunoreactive for vimentin (arrowhead). **e**. The diabetic group (6 days) with a moderate amount of vimentin expression in the intimal and media layers. **f**. The diabetic group (15 days) with a moderate amount of vimentin expression in the intimal and media layers. The scale bar = 10 μm.

days in the diabetic group for both vessel types (arterioles and venules). Figure 3 shows that the IL was immunoreactive for laminin in the CG; however, higher levels of laminin expression were observed in all layers of the vascular wall in the diabetic groups (CG, score 1; DM6, score 2; DM15, score 2). There was no difference in collagen IV staining between the two diabetic groups and the control hamsters. Table 2 shows the distribution scores for cytoskeleton ECM proteins.

## DISCUSSION

Hyperglycemia exerts deleterious effects on the endothelium, which is the regulator of the vascular wall.[3] Abnormalities in the modulatory roles played by the endothelium and/or smooth muscle may be critical and can act as initiating factors in the development of diabetic vascular disease.[18] We observed unaltered endothelium-dependent vasorelaxation at an early stage in STZ-induced diabetes. In our work, the vasorelaxation derived from the endothelium remained unchanged, at least until the 15$^{th}$ day of diabetes development. Our results agreed with those of Pieper (1999),[19] who showed that the vasorelaxation derived from the endothelium increased on the first day after the application of STZ in STZ-induced diabetic rats. This event was followed by a reversal phase (one-two weeks), in which vasorelaxation was normal, and a delayed phase (eight weeks), during which the vasorelaxation became engaged.

Intravital microscopy, which has been extensively used in microcirculation studies, allows *in vivo* measurements of vascular permeability to various compounds.[6] The present study demonstrated the occurrence of changes in microvascular leakage within 2 min after histamine application in diabetic hamsters. Nevertheless, the peak of the response usually occurred 3 to 5 min after histamine application and dissipated within 10 or 20 min. Histamine

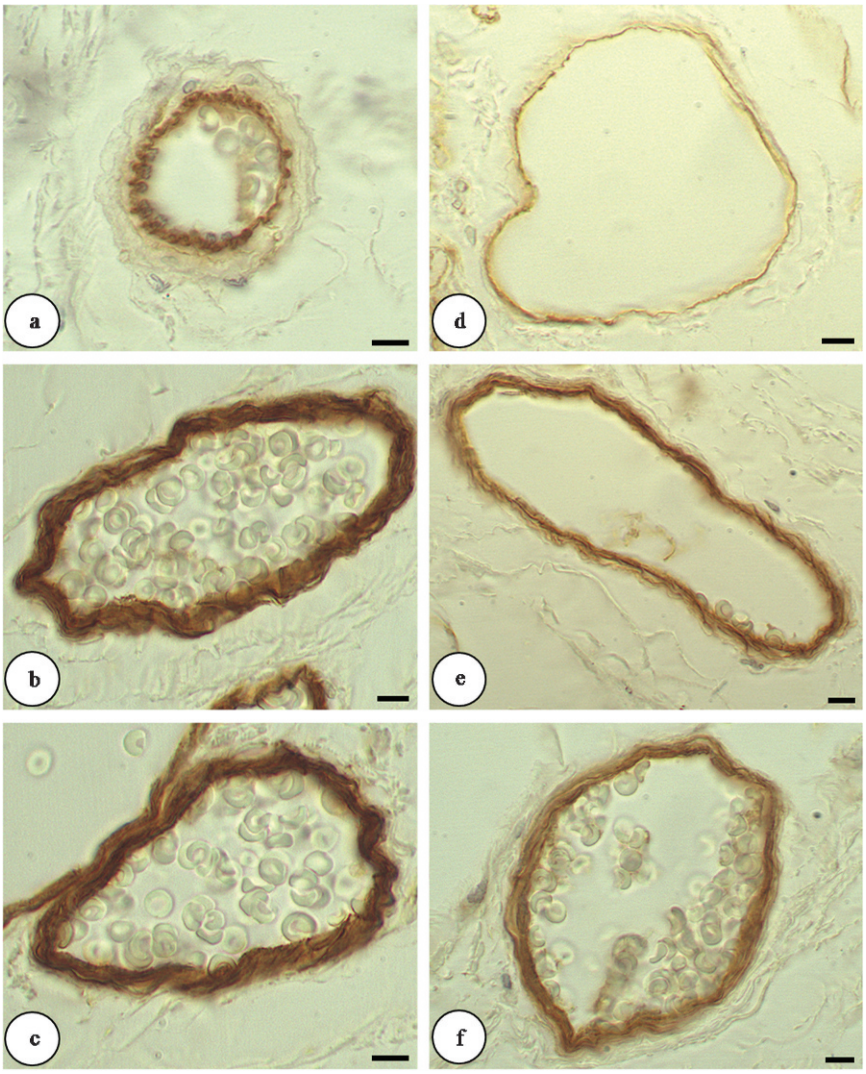


**Figure 3 -** Changes of laminin expression in arterioles (A-C) and venules (D-F) by immunohistochemical staining (light microscopy, 1000X). **a**. The intimal layers of the hamsters in the control group were immunoreactive for laminin. **b** and **c**. All layers showed positive laminin staining for both diabetic groups. **d**. The control group showed a poorly labeled intimal layer. **e**. The diabetic group (6 days) with all layers staining positive. **f**. The diabetic group (15 days) with all layers staining positive. The scale bar = 10 μm.

binding to cell-surface receptors triggers subtle or rapid changes in the contractility of endothelial cells that depends on the cytoskeletal organization and cellular adhesion. Therefore, we can suggest that hyperglycemia influences vascular function at 6 and 15 days of diabetes development and that this change may be associated with subtle changes in the expression and distribution of endothelial cell cytoskeleton components. No significant changes were observed after 5 min of histamine application between the two diabetes groups and the controls. These data agreed with the results of Llorach and coworkers (1976),[20] which did not show alterations in one-two-week diabetic animal models.

Many reports have been published about functional and morphological alterations that occur during the early stage of diabetic disease in multiple animal models. In the present

**Table 2 -** Distribution of actin, talin, α-SMA, vimentin, laminin, and type-IV collagen immunohistochemistry scores in age-matched control and 6- and 15-day diabetic hamsters.

| *Antibodies* | *Control* | | *6 days of diabetes* | | *15 days of diabetes* | |
|---|---|---|---|---|---|---|
| | Arteriole | Venule | Arteriole | Venule | Arteriole | Venule |
| Actin | + | + | ++ | + | + | + |
| Talin | + | + | +++ | + | + | + |
| α-SMA | ++ | + | ++ | +++ | ++ | + |
| Vimentin | + | + | ++ | ++ | ++ | ++ |
| Laminin | ++ | + | +++ | ++ | +++ | ++ |
| Type-IV collagen | ++ | ++ | ++ | ++ | ++ | ++ |

study, no significant changes were observed in morphometric or stereological measurements, in wall thickening or microvessel lumen diameters, in the density of the vessels per cheek pouch area (*QA)* or in volume density (Vv) during the early stage of disease development. Morphological changes require the accumulation of ECM proteins glycated by AGEs[9] and are associated with basement membrane thickening.[14] In part, this thickening may occur when cells synthesize increased amounts of collagen IV.[21] The expression of type-IV collagen, however, did not change in cheek pouch microvessels, which may have resulted from a compensatory mechanism to hyperglycemia in vascular cells that promoted a change in the metabolism of type-IV collagen and increased its turnover. An increase in the turnover of type-IV collagen would avoid accumulation of type-IV collagen and result in a thickening of the basement membrane.

There is some clinical and experimental evidence of augmented blood flow at the early stage of diabetes.[22] Small arteries have the most important influence on local blood flow and are subjected to chemical and neurohormonal influences as well as the continuous effect of mechanical factors generated by the blood stream.[8] The endothelium responds to mechanical stresses through mechanotransduction to regulate the vasomotion and function of the vascular wall. Focal adhesions, which significantly contribute to endothelial cell tethering, mediate the attachment of the actin cytoskeleton to the ECM through a cytoplasmic protein complex (i.e., the focal adhesion plaque).[23] Blood vessel endothelial cells produce focal adhesion molecules, including focal adhesion kinase, vinculin, talin, and cytoskeletal β-actin.

In arterioles, we found that several proteins involved in focal adhesion, such as actin, talin, vimentin, and laminin, were increased in the DM6 group; however, the immunolabels for actin and talin in arterioles were decreased in the DM15 hamsters.

Talin is part of the cytoskeletal protein complex that binds the cytoplasmic tail of integrins to the β-actin cytoskeleton in focal adhesions and is essential for focal adhesion function.[24] Talin is essential for integrin activation, and it is the initial weak link between integrins and the actin cytoskeleton.[25]

Talin,[26] actin and tubulin readily undergo nonenzymatic glycosylation.[27] Loufrani and Henrion (2008)[28] reported that AGEs promote an initial depolymerization of actin filaments (actin F) and a subsequent decrease in actin G expression, which corresponds with a reduction in actin microfilaments and the disruption of cell-cell and cell-matrix junctions. In our study, we used a single antibody to immunolabel both forms of actin; this method could explain the increased expression of actin at 6 days after the onset of diabetes. Talin and actin are key proteins in focal adhesion and represent a mechanical interaction between the cell and the ECM. The force of contraction of the cell is related to focal adhesion.[29] Chronic hyperglycemia produces a nonenzymatic glycation of talin and actin, which may contribute to reduced steady-state adhesion strength and mechanosensing responses. In addition, hyperglycemia can also promote further changes in vascular permeability.

Diabetic hamsters presented increased labeling for laminin in both vessel types. Because laminin is the primary determinant of basement membrane assembly,[30] increased laminin expression may suggest a structural remodeling of vessel basement membranes.

We also found that vimentin was concomitantly increased with laminin expression in blood vessels. All three major cytoskeletal networks have been shown to adapt their structures by elongating their cell shapes and reorienting parallel to the flow direction.[31] Intermediate filament cables, which are initially not under tension, contribute to cell stiffness during large shear deformations. This strain-hardening behavior in the intermediate cytoskeleton filament likely prevents the excessive deformation of the cell at finite strains that would otherwise rupture the actin cytoskeleton.[32] Intermediate filaments may also indirectly interact with focal adhesion sites. Indeed, vimentin intermediate filaments are anchored to α6β4-integrins in microvascular endothelial cells by plectin. Because α6β4 binds to laminin, these interactions are consistent with the hypothesis that intermediate filaments are recruited to provide mechanical stability during physiological adaptation of the microfilament network to hemodynamic shear stress.[31] Thus, the increased expression of vimentin is associated with a proliferative phenotype, possibly due to hyperglycemia.[33] Antibodies against laminin and vimentin inhibit branching morphogenesis in vitro. Therefore, this adhesion structure may play a role in angiogenesis.[34] Like the endothelial cell cytoskeleton, smooth muscle cells are important in maintaining endothelial structural integrity and in regulating endothelial repair.[33]

The expression of α-SMA in venules was enhanced in the DM6 hamsters, and increased expression of α-SMA has been shown to result in increased contractile force generation.[35] In addition, increased expression of α-SMA has been shown to be associated with vessel stability.[32] The primary function of smooth muscle cells (SMC) is the maintenance of blood flow and pressure through their contractility, and α-SMA is necessary for SMC and pericytes to interact with endothelial cells to form a fully functional blood–tissue barrier.[35]

Our results suggest that changes related to cell-matrix interactions occur in response to a new metabolic condition (6 days of a diabetic state). These changes may contribute to pathological remodeling of the microvessels and persist for at least 15 days after the induction of diabetes.

## AUTHOR CONTRIBUTIONS

Silva JF was responsible for the morphometric and stereologic analysis. Carvalho JJ was responsible for the immunohistochemistry assay. Breitenbach MMD was responsible for the induction of diabetes mellitus and data analysis. Cyrino FZGA was responsible for the intravital microscopy of the hamster cheek pouch. Bouskela E participated in the intravital microscopy technique, interpretation of intravital microscopy, immunohistochemistry, analysis of morphometric and stereological techniques, and was responsible for the draft of the introduction, discussion, and conclusions sections.

## REFERENCES

1. Aguiar LG, Villela NR, Bouskela E. [Microcirculation in diabetes: implications for chronic complications and treatment of the disease]. Arq Bras Endocrinol Metabol. 2007;51:204-11.
2. Duling BR, Damon DH. An examination of the measurement of flow heterogeneity in striated muscle. Circ Res. 1987;60:1-13.
3. Schalkwijk CG, Stehouwer CD. Vascular complications in diabetes mellitus: the role of endothelial dysfunction. Clin Sci (Lond). 2005;109:143-59.
4. Meerwaldt R, Links T, Zeebregts C, Tio R, Hillebrands JL, Smit A. The clinical relevance of assessing advanced glycation endproducts accumulation in diabetes. Cardiovasc Diabetol. 2008;7:29.

5. Joyner WL, Mayhan WG, Johnson RL, Phares CK. Microvascular alterations develop in Syrian hamsters after the induction of diabetes mellitus by streptozotocin. Diabetes. 1981;30:93-100.
6. Svensjo E, Cyrino F, Michoud E, Ruggiero D, Bouskela E, Wiernsperger N. Vascular permeability increase as induced by histamine or bradykinin is enhanced by advanced glycation endproducts (AGEs). J Diabetes Complications. 1999;13:187-90.
7. Sotnikova R, Skalska S, Okruhlicova L, Navarova J, Kyselova Z, Zurova J, et al. Changes in the function and ultrastructure of vessels in the rat model of multiple low dose streptozotocin-induced diabetes. Gen Physiol Biophys. 2006;25:289-302.
8. Davies PF. Hemodynamic shear stress and the endothelium in cardiovascular pathophysiology. Nat Clin Pract Cardiovasc Med. 2009;6:16-26.
9. Mott RE, Helmke BP. Mapping the dynamics of shear stress-induced structural changes in endothelial cells. Am J Physiol Cell Physiol. 2007;293:C1616-26.
10. Moncada S. Adventures in vascular biology: a tale of two mediators. Philos Trans R Soc Lond B Biol Sci. 2006;361:735-59.
11. Zhang H, Sunnarborg SW, McNaughton KK, Johns TG, Lee DC, Faber JE. Heparin-binding epidermal growth factor-like growth factor signaling in flow-induced arterial remodeling. Circ Res. 2008;102:1275-85.
12. Jarvisalo MJ, Raitakari M, Toikka JO, Putto-Laurila A, Rontu R, Laine S, et al. Endothelial dysfunction and increased arterial intima-media thickness in children with type 1 diabetes. Circulation. 2004;109:1750-5.
13. Singh R, Barden A, Mori T, Beilin L. Advanced glycation end-products: a review. Diabetologia. 2001;44:129-46.
14. Liu Y, Li H, Bubolz AH, Zhang DX, Gutterman DD. Endothelial cytoskeletal elements are critical for flow-mediated dilation in human coronary arterioles. Med Biol Eng Comput. 2008;46:469-78.
15. Mandarim-de-Lacerda CA. Stereological tools in biomedical research. An Acad Bras Cienc. 2003;75:469-86.
16. Mendonca Lde S, Fernandes-Santos C, Mandarim-de-Lacerda CA. Cardiac and aortic structural alterations due to surgically-induced menopause associated with renovascular hypertension in rats. Int J Exp Pathol. 2007;88:301-9.
17. Bonnet F, Cao Z, Cooper ME, Cox AJ, Kelly DJ, Gilbert RE. Tranilast attenuates vascular hypertrophy, matrix accumulation and growth factor overexpression in experimental diabetes. Diabetes Metab. 2003;29:386-92.
18. Matsumoto T, Oda SI, Kobayashi T, Kamata K. Flow-induced endothelium-dependent vasoreactivity in rat mesenteric arterial bed. J Smooth Muscle Res. 2004;40:1-14.
19. Pieper GM. Enhanced, unaltered and impaired nitric oxide-mediated endothelium-dependent relaxation in experimental diabetes mellitus: importance of disease duration. Diabetologia. 1999;42:204-13.
20. Llorach MA, Bohm GM, Leme JG. Decreased vascular reactions to permeability factors in experimental diabetes. Br J Exp Pathol. 1976;57:747-54.
21. Iglesias-de la Cruz MC, Ziyadeh FN, Isono M, Kouahou M, Han DC, Kalluri R, et al. Effects of high glucose and TGF-beta1 on the expression of collagen IV and vascular endothelial growth factor in mouse podocytes. Kidney Int. 2002;62:901-13.
22. Kobayashi T, Kaneda A, Kamata K. Possible involvement of IGF-1 receptor and IGF-binding protein in insulin-induced enhancement of noradrenaline response in diabetic rat aorta. Br J Pharmacol. 2003;140:285-94.
23. Harrington MA, Daub R, Song A, Stasek J, Garcia JG. Interleukin 1 alpha mediated inhibition of myogenic terminal differentiation: increased sensitivity of Ha-ras transformed cultures. Cell Growth Differ. 1992;3:241-8.
24. Weber E, Rossi A, Solito R, Sacchi G, Agliano M, Gerli R. Focal adhesion molecules expression and fibrillin deposition by lymphatic and blood vessel endothelial cells in culture. Microvasc Res. 2002;64:47-55.
25. Wegener KL, Partridge AW, Han J, Pickford AR, Liddington RC, Ginsberg MH, et al. Structural basis of integrin activation by talin. Cell. 2007;128:171-82.
26. Lee TY, Gotlieb AI. Early stages of endothelial wound repair: conversion of quiescent to migrating endothelial cells involves tyrosine phosphorylation and actin microfilament reorganization. Cell Tissue Res. 1999;297:435-50.
27. Pekiner C, Cullum NA, Hughes JN, Hargreaves AJ, Mahon J, Casson IF, et al. Glycation of brain actin in experimental diabetes. J Neurochem. 1993;61:436-42.
28. Loufrani L, Henrion D. Role of the cytoskeleton in flow (shear stress)-induced dilation and remodeling in resistance arteries. Med Biol Eng Comput. 2008;46:451-60.
29. Lee SE, Kamm RD, Mofrad MR. Force-induced activation of talin and its possible role in focal adhesion mechanotransduction. J Biomech. 2007;40:2096-106.
30. Sasaki T, Fassler R, Hohenester E. Laminin: the crux of basement membrane assembly. J Cell Biol. 2004;164:959-63.
31. Helmke BP. Molecular control of cytoskeletal mechanics by hemodynamic forces. Physiology (Bethesda). 2005;20:43-53.
32. Schopferer M, Bar H, Hochstein B, Sharma S, Mucke N, Herrmann H, et al. Desmin and vimentin intermediate filament networks: their viscoelastic properties investigated by mechanical rheometry. J Mol Biol. 2009;388:133-43.
33. Skalli O, Bloom WS, Ropraz P, Azzarone B, Gabbiani G. Cytoskeletal remodeling of rat aortic smooth muscle cells in vitro: relationships to culture conditions and analogies to in vivo situations. J Submicrosc Cytol. 1986;18:481-93.
34. Gonzales M, Weksler B, Tsuruta D, Goldman RD, Yoon KJ, Hopkinson SB, et al. Structure and function of a vimentin-associated matrix adhesion in endothelial cells. Mol Biol Cell. 2001;12:85-100.
35. Tomasek JJ, Haaksma CJ, Schwartz RJ, Vuong DT, Zhang SX, Ash JD, et al. Deletion of smooth muscle alpha-actin alters blood-retina barrier permeability and retinal function. Invest Ophthalmol Vis Sci. 2006;47:2693-700.